PHYSICAL REVIEW B VOLUME 13, NUMBER 3 1 FEBRUARY 1976

Raman spectra from condensed phases of helium. II. Excitation of more than one phonon

C. M. Surko and R. E. Slusher
Bell Laboratories, Murray Hill, New Jersey 07974
(Received 26 August 1975)

We present Raman spectra for pure solid and liquid ^{3}He, ^{4}He, and $^4\mathrm{He}_x$ $^3\mathrm{He}_{1-x}$ solutions for frequency shifts from 10 to 300 K. The data for all phases show a broad peak. In the solids this peak corresponds reasonably well with the scattering expected from the phonons near the zone boundary. In the liquids a similar interpretation is possible although not compelling. The data from all phases also show a large amount of intensity beyond that corresponding to the maximum of twice a phonon frequency which has a monotonically decreasing dependence on frequency shift. The high-frequency tail extends out to 300 K in the higher density solids (17 cm^3/mole). This feature of the spectra, which is absent in classical solids, is found to correspond to a Raman process where a photon Raman scatters, producing a pair of energetic nearly-free particles with equal and opposite wave vector. The details of this model are explored both theoretically and experimentally.

I. INTRODUCTION

The Raman spectra of solids can be divided into single-phonon and multiphonon processes. Such a division is meaningful in that for the former, a phonon is created with a single well-defined frequency and wave vector; whereas in the latter case several phonons are created, and only the sums of the energies and wave vectors of the phonons are conserved. The preceding paper, which we shall refer to as I,[1] presented an experimental study of the single-phonon Raman spectra of solid helium. These spectra were qualitatively similar to those of other solids, and showed evidence of a well-defined zone-center optic mode. We now present a study of the "multiphonon" Raman spectra of solid and liquid helium.

In most crystals this multiphonon spectrum can be described quite well by considering only two-phonon processes.[2] The spectrum then reflects predominantly the two-phonon joint density of states, and in particular, has a rather sharp decrease in intensity at a frequency shift corresponding to twice that of a zone-boundary phonon. It has been shown previously[3,4] that the multiphonon spectrum of condensed phases of helium is considerably more complicated than this, showing little correspondence to the joint density of states for two phonons and exhibiting spectral weight out to frequency shifts which would correspond to the production of six or eight phonons. In Secs. II–V of this paper we present a detailed study of the multiphonon spectra of pure solid and liquid ^{3}He and ^{4}He and their solutions. We do not consider two-roton scattering in superfluid helium which has previously been studied in detail.[5,6] We present data to demonstrate the extreme similarity of the spectra of all phases of liquid and solid ^{3}He and ^{4}He. We present a simple model which explains the spectral shape and scattered intensity of the spectra at large frequency shifts. We discuss possible interpretation of the "two-phonon" component of the liquid spectra, and the relationship of our data from all phases of helium to the need for a more precise theory of Raman scattering from helium.

II. EXPERIMENTAL APPARATUS

The experimental apparatus and crystal growing and data acquisition procedures used in these experiments are described in detail in I. The solid samples are unoriented. We presume that they are single crystals (at least in the small focal volume collected by the spectrometer) based on the experience of others in growing helium crystals.[7] We do not analyze the polarization properties of the scattered light since we collect a large solid angle of scattered light ($f/3$) and since the sapphire cell windows depolarize incident and scattered light. The spectra shown here were taken with monochromator slit widths of 150 μ, giving a resulting spectral resolution of 3.2-cm^{-1} full width at half-maximum (FWHM). Typical spectra were taken sweeping the spectrometer at a rate of 1 point/sec and averaging 100 such sweeps. The noise in the spectra is predominately statistical, i.e., proportional to the square root of the number of detected photons. Since the frequency shifts of interest are much greater than $kT/\hbar$, where T is the sample temperature, all data shown below correspond to Stokes scattering.

III. EXPERIMENTAL RESULTS

In Fig. 1 is shown the spectrum of a solid hcp $^4\mathrm{He}_{0.8}{}^3\mathrm{He}_{0.2}$ alloy. The sharp feature near 8 cm^{-1} is due to scattering from a single optic phonon. The remainder of the spectrum is due to multiphonon scattering and is prototypical of the spectra

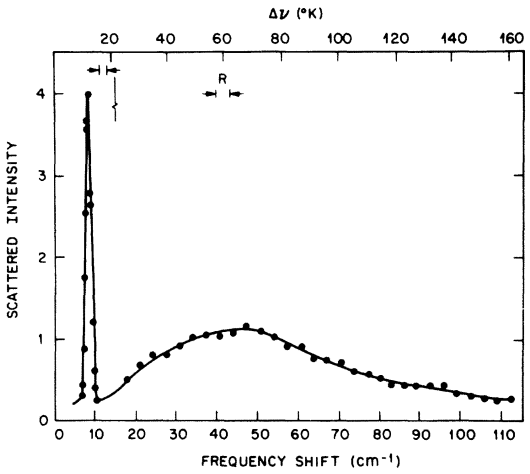

FIG. 1. Raman spectrum of a solid helium alloy $^4He_{0.8}{}^3He_{0.2}$ at 1.4 K and 48 atm pressure. The scattered intensity, in arbitrary units, is plotted as a function of frequency shift. The resolution is 1.2 cm^{-1} FWHM.

of all phases of solid and liquid helium except superfluid ^4He which exhibits an additional sharp peak due to two-roton scattering. For the purpose of this paper, the multiphonon spectrum can be characterized qualitatively by two features: a broad peak and a long monotonically decreasing tail at larger frequency shifts. We will first display the data to study the behavior of the broad peak as a function of isotopic concentration and phase and then show details of the spectrum at larger frequency shifts.

In Figs. 2 and 3 the multiphonon spectra of ^4He and ^3He are shown as a function of molar volume. In the liquid near vapor pressure the peak is at small frequency shifts and there is relatively a large amount of spectral weight near zero frequency. As the molar volume is decreased (by increasing the pressure) the spectral weight at small frequency shifts decreases and the peak shifts to higher frequencies. Qualitatively there is little change upon going from liquid to solid as shown in Figs. 2(c) and 2(d) and in 3(b) and 3(c) or on changing crystal structure in the solid as shown in Figs. 3(a) and 3(b). In Fig. 4 we compare the spectrum of solid ^3He near melting to that of liquid ^3He at the same temperature and nearly the same pressure. The main change in the spectrum is on the low-frequency side of the peak with little if any change in the spectrum at higher frequencies. The spectra are insensitive to changes in temperature in the region from 1.0 to 4.0 K.

Calculations for the two-phonon Raman scattering spectrum in solid helium[8,9] predict peaks in the spectrum due to peaks in the joint density of states. These features are predicted to occur at

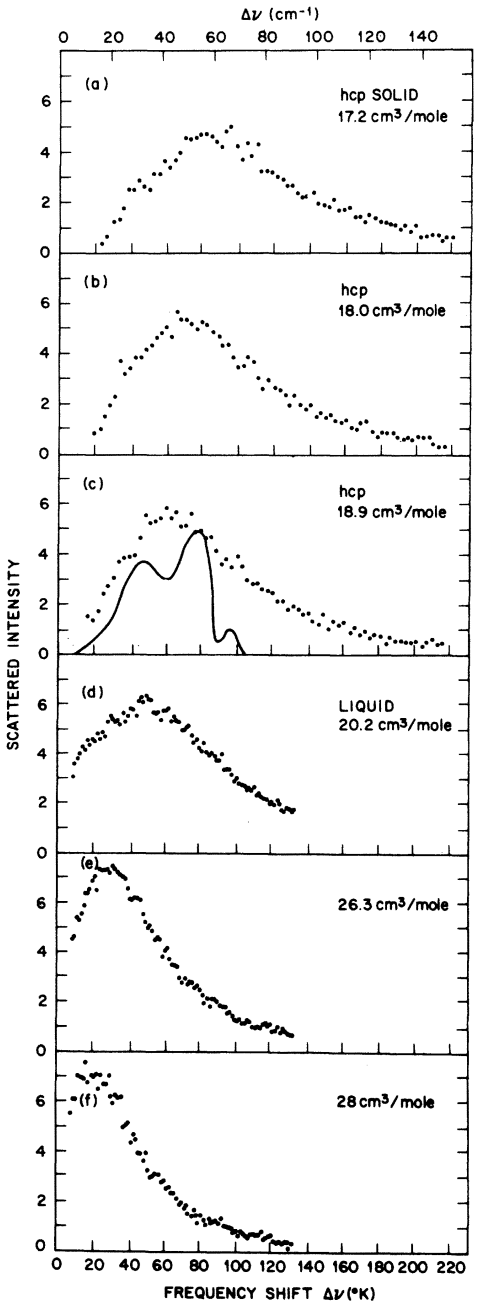

FIG. 2. Multiphonon Raman spectra of solid and liquid ^4He. The temperature is 3.2 K for the liquid spectra and 2.3 K for the solid spectra. The units of scattered intensity are arbitrary but are the same for each spectrum. The resolution is 4 cm^{-1} FWHM.

frequency shifts less than or of the order of that of the peaks in the solid spectra shown in Figs. 2 and 3 and would have widths of the order of 10 cm^{-1}. No consistent and clearly identifiable structure of this type was observed. The slight peak at the frequency shift 43 K in Fig. 2(a) is about as large as any observed. We are unable to assert

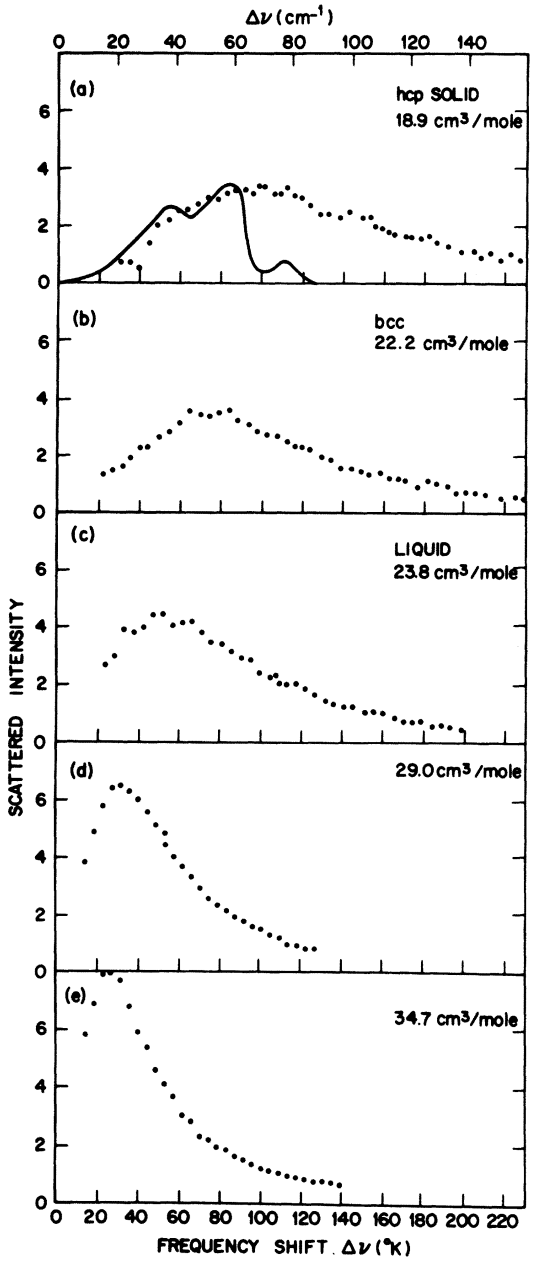

FIG. 3. Multiphonon Raman spectra of solid and liquid ^{3}He at 1.5 K. The units of intensity are arbitrary but are the same for each spectrum. The resolution is 3 cm^{-1} FWHM.

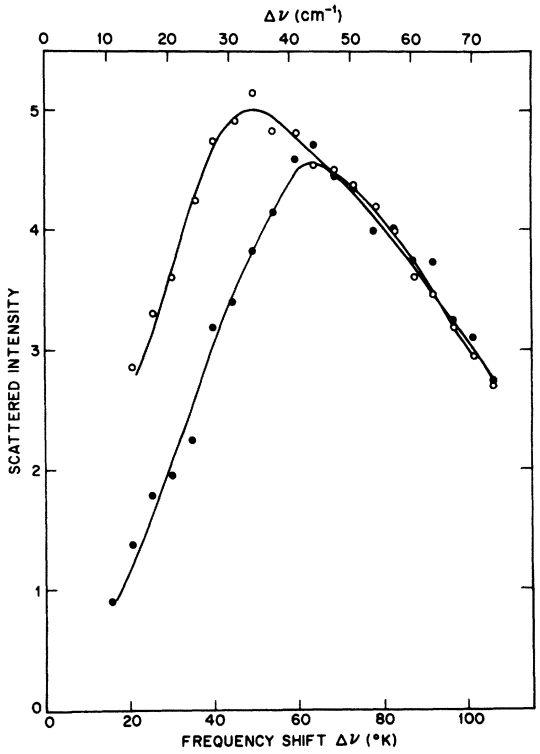

FIG. 4. Raman spectra of solid ^{3}He (solid circles) and liquid ^{3}He (open circles) compared near melting. The temperature is 1.45 K. The pressure is 55.1 atm for the solid and 53.7 atm for the liquid. The resolution is 3 cm^{-1} FWHM. The solid lines are guides to the eye.

that this feature is not due to "noise" although this is somewhat unlikely.

Figures 5 and 6 show the Raman spectral intensity of solid and liquid ^{4}He and ^{3}He at large frequency shifts beyond the broad peak. The data are displayed on a semilogarithmic plot in order to show accurately the spectrum at large frequency shifts. Qualitatively there is little change in the spectrum as a function of molar volume or phase. The derivative of spectral intensity with respect to frequency shift at a given frequency shift $dI(\omega)/d\omega$ decreases as the molar volume is increased. At a given molar volume this quantity is larger for ^{4}He than ^{3}He.

The intensities of the multiphonon spectra in ^{3}He and in ^{4}He relative to spectra of the same isotope at different molar volumes are shown in Figs. 2 and 3. We are unable to ascertain the relative intensities of spectra from different isotopic concentrations at the same molar volume more accurately than to assert that they are equal to within ±30%. The absolute intensity of the multiphonon spectra is obtained by calibration against the measured intensity of the two-roton scattering in superfluid helium. This procedure is described in I for the single phonon intensity. In a similar manner we find the integrated Raman efficiency for the multiphonon spectrum is $(8.5\pm 5)\times 10^{-12}$ cm^{-1} sr^{-1} for the spectrum shown in Fig. 1.

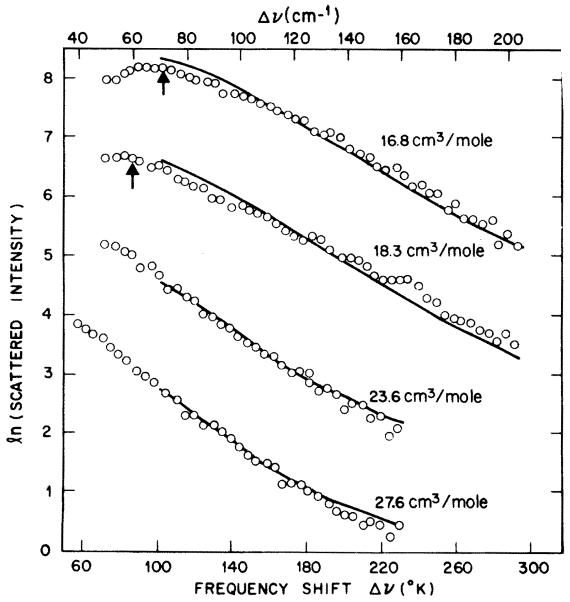

FIG. 5. Semilogarithmic plot of the scattered Raman intensity of ^{4}He at large frequency shifts for different molar volumes. The temperature is 1.5 K and the resolution 3 cm^{-1} FWHM. The upper two curves are for hcp solid and the lower two are for liquid ^{4}He. The data at each molar volume are displaced vertically for clarity. The solid lines indicate the predictions of the model for the free-particle production Raman process. Each curve is translated vertically for best fit. See Table I for comparison of the predicted and measured absolute intensities.

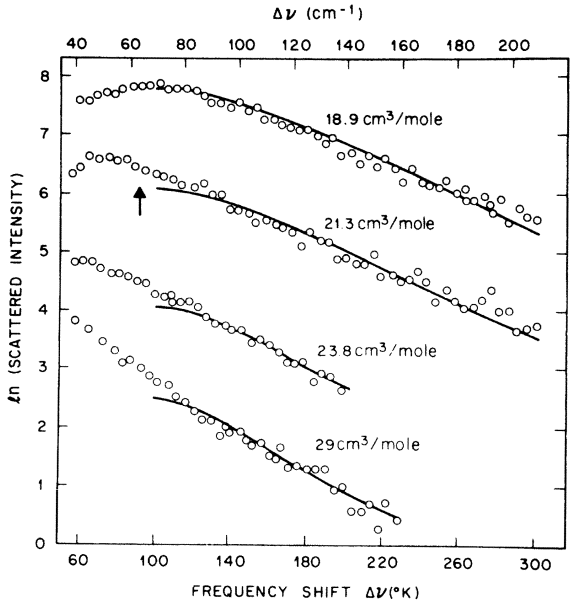

FIG. 6. Semilogarithmic plot of the scattered Raman intensity of ^{3}He at large frequency shifts for different molar volumes. The temperature is 1.5 K and the resolution 3 cm^{-1} FWHM. The upper curve is hcp solid, the next is bcc solid, and the lower two are liquid ^{3}He. The data at each molar volume are displaced vertically for clarity. The solid curves indicated the predictions of the model for the free-particle production Raman process. Each curve is translated vertically for best fit. See Table I for comparison of absolute intensities.

IV. INTERPRETATION OF RESULTS

A. General remarks

The present theories of Raman scattering from helium are not adequate to describe in detail the spectral features of the Raman data shown above. Not only is the theory for classical solids inadequate to explain the solid helium data, but in the case of Raman scattering from liquids there is no theory for either classical or quantum liquids. Therefore in addition to describing the present state of the theories that relate to these measurements, we will discuss the relationship of Raman data from other rare-gas solids and liquids to the helium data presented here.

The theory of Raman scattering from condensed matter involves a description of the modes of atomic motion in the medium and a coupling between these modes and the incident light. For instance, in solid and liquid helium at low frequencies (typically less than the Debye frequency) there are phonon modes. At very high frequencies there is evidence that the "modes" are mainly single-particle excitations.[10,11] In normal (non-superfluid) liquids in addition to the phonons there exist single-particle excitations at arbitrarily low frequencies. The simplest and most common description of the coupling of light to helium is a model where the atoms are replaced by point particles each with a constant polarizability α. The dipole–induced-dipole (DID) interaction is used to describe the coupling of the incident light to modes in the medium giving rise to Raman scattering. Recently quantum-mechanical calculations have been carried out for the polarizability of pairs of helium atoms.[12] These calculations show that the DID model describes the pair polarizability to better than 50% for internuclear separations relevant to liquid and solid helium. Thus the DID model is a reasonable approximation, and furthermore the quantum calculations provide a more rigorous basis for a refined theory. The DID model has been the basis of calculation of Raman scattering from both solid and superfluid helium.[8,13,14] While both predictions are inadequate to describe the data in detail they provide at least qualitative insight into the multiphonon Raman processes.

B. Multiphonon peak

The calculation done by Werthamer, Koehler, and Gray[8] for solid helium uses DID coupling and

phonon modes calculated from self-consistent phonon theory to calculate scattering from one and two phonon processes. For an n phonon process with $n \geq 2$, the integrated intensity is expected to be proportional to $(u/a)^{2n}$ (where u is the amplitude of the zero-point motion of an atom and a is the lattice spacing), so that for helium where $u/a \simeq 0.3$ it is expected that higher-order (e.g., three-phonon) processes will be relatively unimportant. Their calculation describes semiquantitatively the Raman spectrum of solid Ar, Kr, and Xe, where little spectral weight is measured beyond the frequency for production of two phonons.[15] In Xe the fine structure in the spectra due to peaks in the density of states for particular combinations of phonon branches has been resolved, and these measurements[15] agree with the theoretical predictions. The theoretical predictions for solid hcp helium at approximately 19 cm^3/mole are shown by the solid lines in Figs. 2(c) and 3(a).[8,9] The theory predicts roughly the correct position of the broad peak but cannot account for the large amount of spectral weight at frequencies corresponding to more than two phonons. The peak in the calculated spectrum arises from the large contribution of the two-phonon joint density of states near the zone boundary. Neutron scattering measurements in ^{4}He indicate that the phonons are well defined with frequency position-to-width ratios in all cases

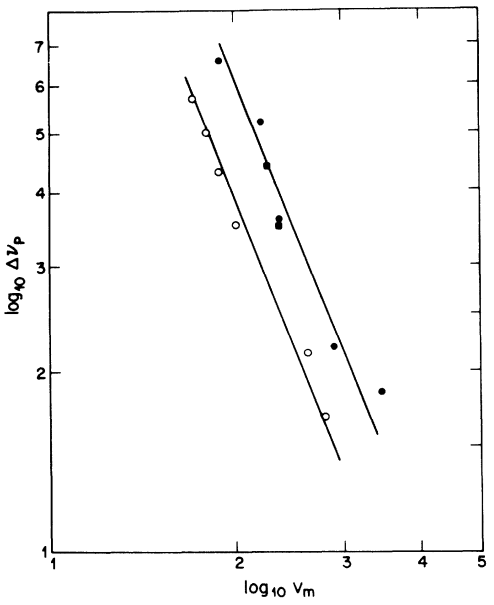

FIG. 7. Peak position of the multiphonon Raman spectra is plotted as a function of molar volume. The open circles are taken from the ^{4}He data in Fig. 2. The solid circles and squares are ^{3}He data taken from Figs. 3 and 4, respectively. The solid lines correspond to a Grüneisen parameter of 2.6.

greater than three, so that phonon damping is not expected to modify appreciably the theoretical calculation of the two-phonon spectra (which assumes undamped excitations). In order to study the contribution of two-phonon scattering to the observed peak, we plot in Fig. 7 the molar volume dependence of the peak position in solid and liquid helium. Shown for comparison is a line which corresponds to a Grüneisen parameter $(d\ln\omega/d\ln V)$ of 2.6. This value corresponds to the molar volume dependence of phonon frequencies consistent with the optic-phonon measurements presented in I, with the measurements in ^{4}He by neutron scattering, and with specific-heat measurements.[16] The fact that the Raman peak scales with phonon frequencies is consistent with the interpretation that this peak is due to phonon scattering. The fact that the peak frequency agrees reasonably well with the theory indicates that the peak is due to two-phonon processes. We will discuss in detail below contributions to the spectral weight at higher frequencies.

The observed scattered intensity from the two-phonon spectrum agrees within a factor of three with the DID model. The theory would predict a Raman scattering efficiency of 3×10^{-11} $cm^{-1}sr^{-1}$ for the spectrum in Fig. 1 as compared with the measured value of 8.5×10^{-12} $cm^{-1}sr^{-1}$. The predicted value would be decreased if atomic overlap corrections to the pair polarizability were included. This correction is described in Eq. (2) below with respect to a different feature of the spectrum.

While the broad peak in the solid can be understood in terms of conventional phonon theory, there is less known about modes in the liquid. The fact that the spectrum is qualitatively unchanged upon going from solid to liquid (see Fig. 4) is the strongest argument for similar "zone-boundary phonon" modes in the liquid. Much of the shift in peak position upon melting can be attributed to the molar volume change. The rest of the apparent shift in peak position appears to be caused by an increase in scattering at low frequencies. In the nonsuperfluid phases of liquid helium the increased scattered intensity at small frequency shifts becomes increasingly apparent as the molar volume of the liquid is decreased. In superfluid helium this spectral weight at small frequency shifts is completely absent. It is likely that the main contribution to the spectral weight at small frequency shifts is due to pairs of single-particle excitations at small momenta which are not present in superfluid helium.

As has been pointed out previously,[3,4] the peak in the liquids is consistent with the existence of well-defined modes extending out to the zone

boundary, where they produce a peak in the density of states for the production of two phonons. Such modes have been predicted for normal liquid helium[17] and have been predicted and observed in some but not all classical liquids.[17,18] A recent calculation by Aldrich and Pines[19] predicts the energy and wave-vector dependence of these excitations in liquid ^{3}He. A comparison of the value of frequency shift which corresponds to a maximum in the joint density of states yields a predicted peak position of 36 and 39 cm^{-1} at 35 and 29 cm^3 molar volumes as compared with the respective measured peak positions of 27 and 32 cm^{-1}. The agreement is moderately good considering this comparison neglects any wave-vector dependence of the coupling of light to the modes. As shown in Fig. 7, the molar volume dependence of the peak position in the liquid is also consistent with the "phonon" interpretation. This is the strongest evidence for a high-frequency collective excitation in liquid ^{3}He. In ^{3}He, the "roton" portion of the excitation curve is probably damped by single-particle excitations, but it is expected that the "maxon" will remain underdamped.

We conclude that the broad peak evident in the Raman spectra of all phases of helium is most likely due to scattering from pairs of excitations whose wave vector is approximately π/a where a is the average interparticle spacing. In the solids these excitations are zone-boundary phonons. In the liquids these excitations are the analogous high-frequency collective modes (i.e., maxons) predicted by Pines.[17]

C. Spectra at large frequency shifts

Having discussed the multiphonon spectrum in the region of the broad peak we now discuss the spectrum at larger frequency shifts where the spectra from all phases of helium show an intensity which decreases monotonically as a function of frequency shift. This feature of the Raman spectra in solid helium is absent in the spectra of the heavier rare-gas solids where the integrated Raman intensity in the frequency range beyond that for the production of two phonons is less than 0.01–0.1 of the total Raman intensity[15] (depending on the temperature). In contrast to this, for helium this ratio ranges from 0.3 to 0.6 depending on the phase. The spectra of heavier rare-gas liquids are not easily compared with that for helium since, for the former, $\hbar\omega \approx kT$ in the frequency region of interest. This makes description of the initial and final states of the system more difficult.

We now develop a simple model calculation with which we are able to describe quantitatively the Raman spectra at large frequency shifts in all condensed phases of ^{3}He and ^{4}He. We calculate the Raman process where incident light with energy $\hbar\omega_0$ creates a pair of nearly-free-particle excitations, each with equal and oppositely directed wave vector $\vec{\kappa}$ and energy $\epsilon_{\vec{\kappa}}$, and a scattered photon of energy $\hbar\omega_0 - 2\epsilon_{\vec{\kappa}}$. Consideration of this process is motivated by the fact that the excitation spectrum of helium at large energies (>30 K) and large momenta (>2.5 $Å^{-1}$) is dominated by spectral weight centered around the dispersion relation

$$\epsilon_{\vec{\kappa}} = \hbar^2\kappa^2/2m^*, \tag{1}$$

where m^* is close to the "bare" particle mass m. These free-particle excitations have been observed by neutron scattering in both liquid and solid ^{4}He.[10,11] That they appear in helium at such low energies, comparable to or slightly greater than a zone-boundary phonon, is due to the weak attractive nature of the helium potential and the large zero-point motion which tends to expand the lattice. Thus when a helium atom is given an energy greater than the moderately small energy necessary to remove it from its lattice site ($\epsilon \gtrsim$ 40 K), it can travel for some distance (>1 Å) before interacting strongly with another atom.[20] Neutron scattering can produce one single-particle excitation of this type, but the lowest-order process allowable with light scattering is two excitations with nearly equal and oppositely directed wave vector since the photon has negligible small wave vector on this scale. This process can also be viewed as the production by an incident photon of a "particle-hole pair" and a scattered photon, since at these large momenta a "hole" excitation is equivalent to an excited particle moving in the opposite direction.

The polarizability of a pair of helium atoms has recently been calculated quantum mechanically to include effects produced by overlap of the electron wave functions.[12] This calculation provides an accurate basis for our model of the Raman production of single-particle excitations, a process which is found to be sensitive to the interaction at short distances where overlap effects are most important. The result of the calculation for the anisotropic part of the pair polarizability $\vec{\beta}(\vec{r})$ may be written

$$\vec{\beta}(\vec{r}) = (6\alpha_0^2/r^3)(3\hat{r}\hat{r} - \vec{I})\gamma(r), \tag{2}$$

where α_0 is the atomic polarizability and $\vec{r}$ is the separation vector between atoms. The quantity $\gamma(r)$ has a value of unity at large distances $|\vec{r}| \gtrsim 3.2$ Å, where the interaction may be described classically by a dipole–induced-dipole (DID) model, and decreases as r decreases to the value of 0.5 at $r = 1.8$ Å (which is effectively the shortest distance of approach relevant to our highest density solid).

We use $\vec{\beta}(\vec{r})$ from Eq. (2) and perturbation theory to calculate the Raman scattering process where an energetic pair of nearly-free particles is produced in the final state. The Hamiltonian is $H = -\frac{1}{2}\vec{E}\cdot\vec{\beta}(\vec{r})\cdot\vec{E}$, where $\vec{E}$ is the sum of the electric fields of incident and scattered light. The Raman efficiency at frequency shift ω (which is defined as the scattering rate per unit solid angle, per unit frequency shift, per unit incident photon flux, per unit length of the sample) is found to be

$$R_{\vec{\lambda}_0\vec{\lambda}_s}(\omega) = \frac{\hbar k_0^4}{V^2}\sum_f |\langle f|\vec{\lambda}_0\cdot\vec{\beta}(r)\cdot\vec{\lambda}_s|i\rangle|^2 \times \delta(\epsilon_{fi} - \hbar\omega), \quad (3)$$

where k_0 is the wave vector of the incident light with polarization direction $\vec{\lambda}_0$, $\vec{\lambda}_s$ is the polarization of the scattered photon, ϵ_{fi} is the energy difference between initial and final states $|i\rangle$ and $|f\rangle$, and V is the interaction volume. If we take the initial state to be spherically symmetric, write the final particle states in terms of plane waves of momentum κ and take $\lambda_0 \perp \lambda_s$ (since our experimental arrangement collects depolarized scattering only), we find

$$R_{\lambda_0\lambda_s}(\omega) = \frac{\hbar k_0^4}{V}\sum_\kappa \frac{(24\pi\alpha_0^2)^2}{V}(\kappa_{\lambda_0}\kappa_{\lambda_s})^2 \times\left|\int j_2(\kappa r)\psi_i(r)\gamma(r)\frac{dr}{r}\right|^2 \delta(\epsilon_{fi}-\hbar\omega), \quad (4)$$

where $j_2(\kappa r)$ is a spherical Bessel function of order 2, and $\psi_i(r)$ is the initial-state wave function. We take the final-state particles with wave vector κ to be distributed about the energy $\hbar^2\kappa^2/2m^*$ in a Gaussian manner with a $1/e$ width $\Gamma\hbar\kappa$ which is linearly proportioned to κ. This distribution treats phenomenologically the effect of the medium on these nearly-free particle states. The width accounts for both the initial velocity distribution of the particles and the lifetime broadening of the final state (which is most important for $\kappa < 80$ Å^{-1}).[20] The effective mass m^* treats the effect of the medium on the real part of the final-state energy. It is known from neutron experiments to be different from the bare-particle mass in the energy region of interest for solid ^{4}He. The assumption of a Gaussian distribution for the particle energies is reasonably consistent with neutron measurements. In fact we are interested in a convolution of particle distributions at κ and $-\kappa$, and this function is fit very well by a Gaussian distribution.

The initial-state wave function ψ_i is taken from measured values of the pair correlation function

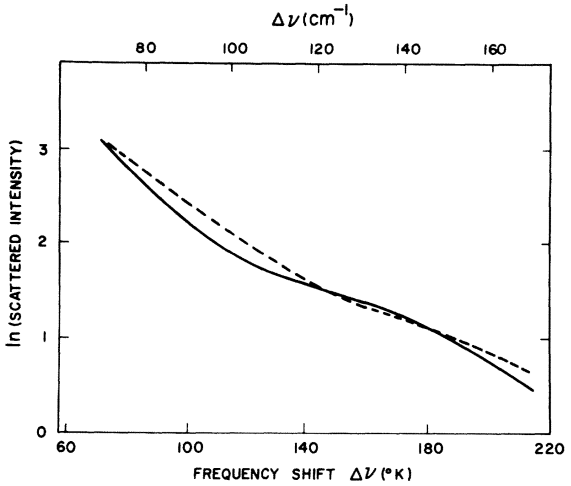

FIG. 8. Dependence of the model calculation on the width parameter Γ for liquid ^{4}He at 27.6 cm^3/mole. The dashed curve is for the value of $\Gamma = 11.2$ K/Å^{-1} used in the calculation. The solid line is for $\Gamma = 8.7$ K/Å^{-1}, which corresponds to the best fit to the neutron data.

$g(r)$ in liquid helium[21] and from calculated values of the "short-range correlation function" in solid helium.[22] Thus in the liquids we identify

$$\psi_i(r) = g^{1/2}(r). \quad (5)$$

We note that with this identification our expression for $R_{\lambda_0\lambda_s}$ is similar to that of Baeriswyl[23] with the exceptions that $g(r)$ (which was inserted *ad hoc* by Baeriswyl) is found to be replaced by $\gamma(r)g^{1/2}(r)$ and that our expression treats scattering from "single-particle" excitations rather than collective elementary excitations. We discuss below the error introduced by assuming a spherically symmetric $\psi_i(r)$ and a plane-wave final-state wave function.

The resulting predictions for the spectra at large frequency shifts are shown by the solid lines in Figs. 5 and 6. Values of Γ and m^* were taken from neutron measurements on[10,11,20,24] ^{4}He and are scaled in density according to a straight-line fit on a logarithmic plot of Γ and m^* as functions of the molar volume V_m. The values of Γ used for these spectra were increased 30% above those values indicated by the neutron data. Both values of Γ showed the same integrated intensity and average slope on a semilogarithmic plot of intensity as a function of frequency shift but the smaller value showed more of the frequency-dependent structure of the matrix element than is observed in our experiment. The effect of this change in Γ for the parameters relevant to liquid ^{4}He at 27.6 cm^3/mole is shown in Fig. 8. For ^{3}He we scale from ^{4}He according to $m_3^*(V_m) = \frac{3}{4}m_4^*(V_m)$ and $\Gamma_3(V_m) = \frac{4}{3}\Gamma_4(V_m)$ (Ref. 20) (which is consistent with lifetime broad-

TABLE I. A comparison of the experimental Raman scattering intensities I_{ex} measured at a frequency shift of 115 cm^{-1} and a resolution of 3 cm^{-1} (FWHM) and the corresponding theoretical intensities I_{th} calculated from the model described in the text at various molar volumes for both ^4He and ^3He.

Isotope	V_m (cm^3/mole)	I_{ex} (counts/sec)	I_{th} (counts/sec)	I_{ex}/I
^4He	27.6	0.42	0.41	1.03
^4He	23.6	0.68	0.71	0.96
^4He	18.3	1.3	1.16	1.12
^4He	17	1.7	1.8	0.95
^3He	29	0.41	0.38	1.08
^3He	23.8	0.89	0.57	1.56
^3He	21	1.12	0.81	1.38
^3He	18.9	1.69	0.97	1.70

ening of the final state being the dominant contribution to Γ). The experimental and theoretical values for the correlation functions which we take for $\psi_i(r)$ were shifted up to 0.2 Å to account for changes in V_m. In Figs. 5 and 6 the intensity of the calculated spectrum at each molar volume is adjusted for best fit with the data by shifting the calculated curves vertically with respect to the data. We discuss below comparison of the absolute intensity. We regard the general agreement between theory and experiment to be strong evidence that "nearly-free-particle pair production" dominates the Raman scattering from helium at large frequency shifts. The arrows in Figs. 5 and 6 indicate the maximum frequency for the production of two phonons in the solids. From the results of neutron studies on ^4He,[10,11] we expect that at frequency shifts smaller than this the free-particle process will become less important than two-phonon Raman scattering. The transition is likely to be complicated and our calculation ceases to apply when the dynamic structure factor $S(\kappa, \omega)$ has appreciable weight in other than free-particle modes.

In Table I we compare the measured intensity in the high-frequency tail with the predictions of our model. The intensities shown are for 3-cm^{-1} resolution (FWHM) at a frequency shift of 166 K and correspond to the spectra shown in Figs. 5 and 6. The agreement is excellent for ^4He and reasonably good for ^3He, considering our lack of knowledge of $\psi_i(r)$. To our knowledge this is the most accurate prediction for scattered intensities of the Raman spectra of condensed phases of helium. This agreement gives us further confidence in the assertion that at large frequency shifts, the Raman scattering is dominated by the nearly-free-particle Raman process described here.

This model is appropriate for helium where the system is loosely packed and the "well depth" of the potential binding an atom to a particular site is comparable to or less than the frequency of excitations. The model would be appropriate for H_2 and the heavier rare gases[15,25] but only at much higher frequencies than those corresponding to the maximum energy for the production of two phonons, since in these systems the attractive potential binds an atom much more strongly to a lattice site than the energy necessary to create a zone-boundary phonon. For example, the binding energy E_b amounts to 41 K in He in contrast to 715 K in Ar,[26] whereas the Debye temperature Θ_D is 18 and 93 K, respectively. For the heavier rare-gas solids we have calculated the Raman intensity for the production of an energetic pair of free particles using Eq. (3) and an initial-state wave function corresponding to atoms allowed to make random "zero-point-motion" excursions of amplitude $\langle u^2\rangle^{1/2}$ about fixed lattice sites. The resulting spectrum for this process $I(\omega)$, valid for $\hbar\omega > 2E_b$ and $\langle u^2\rangle^{1/2}/a \ll 1$, is found to be

$$I(\omega) = Ce^{-\hbar\omega/\Theta_D}, \tag{6}$$

where we have assumed a Debye phonon spectrum, Θ_D is the Debye temperature, and C is a constant depending on the particular substance. The frequency dependence of Eq. (6) is of the form of the Debye-Waller factor $e^{-\kappa^2\langle u^2\rangle/2}$. For argon, C is found to be approximately 15 times the maximum two-phonon intensity. Thus in the frequency interval $\hbar\omega > 2E_b$ where Eq. (6) is valid, $I(\omega) < 15e^{-2E_b/\Theta_D} < 10^{-5}$ of the maximum two-phonon intensity.

It is our claim that this is the first calculation of the Raman intensity from helium which treats properly the interaction at small distances. We have removed the need for a phenomenological cutoff of the interaction used in previous calculations.[13,14,23] Since this "cutoff" affects drastically the predicted intensity and spectral shape, the calculation presented here is a significant step toward predicting absolute intensities for Raman scattering from helium. It is also the first reliable calculation of the spectral shape over any extended frequency interval. The model only applies

at large frequency shifts however, and it would be very desirable to develop a more complete theory valid at arbitrary frequency shifts. This is particularly relevant for the case of superfluid helium where details such as prediction of the scattering intensity for two maxons or the absolute intensity for two-roton scattering are beyond the capabilities of present theories. It is only the very narrow region of frequencies over which the two-roton scattering extends which allows calculation of the spectral shape. It is assumed in the superfluid case that the matrix element is constant and that the shape is dominated by variations in the joint density of states and by roton-roton interaction effects.

We have investigated the effect of using a nonspherically symmetric initial-state wave function ψ_i. We have taken a ground-state wave function modeled by Gaussians centered on a bcc lattice with a Jastrow function to cutoff the two-body wave function at short distances. We then compare the square of the matrix element, summed over the possible directions of κ, computed using this "solid" wave function with that computed using a spherical average of the same ψ_i. The matrix elements are found to be similar in κ dependence and within 30% in magnitude. These results indicate that the spherical average wave function is a reasonable approximation. The assumption of a plane-wave final-state wave function is justified by the fact that the two-body helium potential changes very little compared to ϵ_κ in the range of internuclear separations where $\psi_i \neq 0$. The hard core cuts off $\psi_i(r)$ at a value of r large compared to that at which the hard-core potential would modify the final-state wave function.

CONCLUSION

The Raman spectra of pure solid and liquid ^{3}He and ^{4}He are shown to be qualitatively very similar. Other than the sharp feature in superfluid helium due to two-roton scattering and scattering from the single optic phonon in the hcp phases of the solids, the spectra are characterized by a broad peak followed by monotonically decreasing intensity extending to much larger frequency shifts. We identify the broad peak as due to scattering from two excitations near the "zone boundary" (i.e., with wave vector approximately equal to π/a, where a is the average interparticle spacing). We identify the spectrum at larger frequency shifts as a Raman scattering process where incident light at frequency ω_0 creates an energetic pair of nearly-free particles with equal and opposite wave vector and a scattered photon. We have calculated the Raman scattering expected for this process and have shown that it agrees quantitatively with our measurements. This model should be of use in studying of the two-body ground-state wave function in ^{3}He and ^{4}He.

ACKNOWLEDGMENTS

We wish to acknowledge helpful conversations with P. B. Allen, J. I. Gersten, C. Herring, C. M. Varma, and N. R. Werthamer.

---

[1]R. E. Slusher and C. M. Surko, preceding paper, Phys. Rev. B 13, 1086 (1976).
[2]For example, see S. L. Cunningham, J. R. Hardy, and M. Hass in *Light Scattering From Solids*, edited by M. Balkanski (Flammarion, Paris, 1971).
[3]R. E. Slusher and C. M. Surko, Phys. Rev. Lett. 27, 1699 (1971); C. M. Surko and R. E. Slusher, in *Low Temperatures Physics -LT13*, edited by K. D. Timmerhaus, W. J. Sullivan and E. F. Hammel (Plenum, New York, 1974), Vol. 2 pp. 100–104.
[4]E. R. Pike and J. M. Vaughan, J. Phys. C 3, L90 (1972).
[5]R. L. Woerner, D. A. Rockwell, and T. J. Greytak, Phys. Rev. Lett. 30, 1114 (1973), and references therein.
[6]C. M. Surko and R. E. Slusher, Phys. Rev. Lett. 30, 1111 (1973).
[7]A. F. Schuch, in *Low Temperature Physics and Chemistry*, edited by J. R. Dillinger (University of Wisconsin, Madison, 1958), p. 79.
[8]N. R. Werthamer, R. L. Gray, and T. R. Koehler, Phys. Rev. B 4, 1324 (1971).
[9]The solid lines in Figs. 2(c) and 3(a) are the predictions of Ref. 8 for the spectral shape relevant to the parameters of our experiment. An equally weighted average is taken over the possible crystal orientations.
[10]R. A. Cowley and A. D. B. Woods, Can. J. Phys. 49, 177 (1971).
[11]V. J. Minkiewitz, T. A. Kitchens, G. Shirane, and E. B. Osgood, Phys. Rev. A 8, 1513 (1973).
[12]D. W. Oxtoby and W. M. Gelbart, J. Mol. Phys. (to be published).
[13]M. J. Stephen, Phys. Rev. 187, 279 (1969).
[14]A. L. Fetter, J. Low Temp. Phys. 6, 487 (1972).
[15]P. S. Fleury, J. M. Worlock, and H. L. Carter, Phys. Rev. Lett. 30, 591 (1973).
[16]See Sec. III A of I, and references therein.
[17]D. Pines, in *Quantum Fluids*, edited by D. F. Brewer (North-Holland, Amsterdam, 1966), pp. 257–266.
[18]J. R. D. Copely and J. M. Rowe, Phys. Rev. Lett. 32, 49 (1974).
[19]C. H. Aldrich, Ph.D. thesis (University of Illinois, 1974) (unpublished); and C. H. Aldrich and D. Pines (unpublished).
[20]V. F. Sears, Ber. Otsch. Bunsenaes Ges. 75, 376 (1971).

[21]E. K. Achter and L. Meyer, Phys. Rev. 188, 291 (1969); R. D. Mountain and H. J. Raveche, J. Res. Natl. Bur. Stand. (U. S.) A 77, 725 (1973).
[22]H. R. Glyde and F. C. Khanna, Can J. Phys. 49, 2997 (1971).
[23]D. Baeriswyl, Phys. Lett. A 41, 297 (1972).
[24]V. F. Sears, Solid State Commun. 11, 1307 (1972).
[25]P. A. Fleury and J. P. McTague, Phys. Rev. Lett. 31, 914 (1973); Phys. Rev. A 12, 317 (1975).
[26]R. A. Guyer, *Solid State Physics* (Academic, New York, 1969), Vol. 23, pp. 413–499; in particular, see Table III, p. 424.